Master Thesis

Towards lifelong mapping in pointclouds

Panagiotis Chatzichristodoulou

Master Thesis DKE 09-16

Thesis submitted in partial fulfillment
of the requirements for the degree of Master of Science
of Artificial Intelligence at the Department of Knowledge
Engineering of the Maastricht University

Thesis Commitee:
University of Maastricht
Rico Mockel, Kurt Driessens
Dobots B.V.
Anne Van Rossum

Maastricht University
Faculty of Humanities and Sciences
Department of Knowledge Engineering
Master Articial Intelligence

June 21, 2015

Abstract

Long term mapping is the natural extension to existing mapping methods. Mapping an area for a large amount of time is a problem that if tackled efficiently will be a large step towards highly autonomous robots. As discussed in the literature lifelong mapping consists of two major subproblems. A compression, and a dynamic environment problem. The thesis discuses the application of non parametric Bayesian methods and how such tools can be directed to improve lifelong mapping capabilities of existing methods. A novel method of object clustering, point cloud representation and feature matching is presented and its results are applied to an EKF SLAM algorithm; its strengths, weaknesses are analysed as well as future directions on how the method could be improved as well as extended to be able to cope with dynamic enviroments.

Contents

List of Figures

List of Tables

1. Introduction

Simultaneous localization and mapping is one of the fundamental problems of autonomous systems[1]. In order for a robot to be considered truly autonomous, it must have the ability to enter an area and infer its structure. To that direction, a lot of effort has been put in algorithms that are able to map static environments. With solutions like EKF-SLAM[2], FastSlam[40] and GraphSLAM[3] robots are now able to efficiently map static environments. The logical extention to methods that can map static environments is methods that remove this restriction. The idea of lifelong robot learning is not new and has been introduced as a general concept to the literature by Sebastian Thrun [5]. Konolige et al.[6] specifically focus on lifelong learning in mapping and the utility such methods would have. In the PhD thesis of Walcott [7] long term mapping is decomposed to 4 basic subproblems:

- Continuously incorporate new information.
- Address the problem of tractability for growing DPG
- Representation of the environment should include the history of the map as changes occur with the passage of time.
- Detect changes and update the map online

The first two problems can be though of as compression problems as the map increases over time whereas the latter ones can be though of as dynamic environment one. Approaches of tackling those problems vary according to the sensors a robot is using to perform the mapping. In this project the focus will be directed towards methods that use RGBD devices like Microsoft's Kinect to perform SLAM.

Since its introduction in 2010 Microsoft Kinect[25] has revolutionized RGBD devices with its low price range and high quality sensors. It came as no surprise that research in point clouds, the representation system of Kinect, has increased since then. Many libraries that enable the user to perform tasks from feature extraction to plane segmentation[12] in pointclouds are currently available. In the field of robotics, many teams are using the Kinect sensors to perform simultaneous localization and mapping[13]. The goal of this thesis is to introduce a novel approach to tackle the compression problem of long term mapping methods that use the Kinect devices while using Bayesian non parametric methods as the base of its solution.

Dirichlet processes and Dirichlet process mixture models [26] are the cornerstone of Bayesian non parametric statistics. The strength of those models lies in the fact that they allow the model's mixture components to grow as much as needed so as to best fit the data. The dynamic number of components in combination with many different prior choices lead to very flexible models that can be used in a very large area of applications from topic modeling[43] to speaker diarization[45].

The main motivation behind this project is to use such methods as a means of compressing the information provided by the environment. In that direction, finding a way to robustly cluster a point cloud into "chunks" of structure seems a reasonable starting point. This leads to the direction of object based SLAM, which is a domain where objects are used as reference points to perform the mapping.

In this paper, an EKF SLAM method that uses point clouds as input will be implemented. More specifically, a landmark detection layer will be incroporated; its results will then be empirically

tested as well as its ability to optimally compress the data of a point cloud. Its strengths and weaknesses will be presented and analysed; furthermore, directions on how the method could be extended to tackle the first two subproblems of Walcott's thesis will be given in the discussion.

The rest of the paper is structured as follows. Section 2 will present relevant literature review, Section 3 will introduce the theories behind the model, Section 4 will define the model, Section 5 will show experimental results of the method. Finally, Section 6 will end up with a discussion on the methods strengths and weaknesses.

2. Literature review

Related research will be focused on 4 general sub fields of related literature.

- Object based SLAM or semantic slam
- Point Cloud Object segmentation
- Non-parametric clustering methods
- The correspondence problem in SLAM

Due to the fact that point clouds are used as input and from such input object representations must be extracted, methods that use such approaches to perform SLAM are then needed. Object based SLAM methods are therefore important due to the nature of the input at hand. The second part of the research is focused on point cloud representations. This part of the research is mostly focused on what features or meta-features need to be taken into account so that the reduced representation is solid. The third part of the research is focused on non-parametric Bayesian methods and the clustering tools they provide. Such tools are important as they can be used to provide new approaches to object segmentation within a point cloud. Finally, research is focused on the correspondence problem in SLAM. As one of the fundamental problems that need to be solved in order to have robust SLAM algorithms, it is imperative the correspondence problem be solved efficiently. In that extent and due to the unique representation of our objects, a novel approach that takes elements from other techniques in the correspondence between objects in a SLAM problem is given.

2.1. Object based SLAM

Object based SLAM or semantic slam methods proposed in the literature focus at domain specific solutions of particular problems. Salas-Moreno et al [14] define a method of performing object based slam for specific objects. The objects are identified by camera that is on top of the robot. By having a model of pre-trained objects, SLAM can be performed on environments the robot knows what objects to expect. The disadvantage of that method is that object models have be to be well defined and there is a small number of such objects. Castle et al. use object recognition to perform object based SLAM with the use of a hand-held cameras. Selvatici et al [15] use a similar approach while exploiting structural information such as object height and position within the room. That way a couch that is a large object situated in floor level is easier to be recognized. Choudhary et al. [17] use point clouds and an object database to match objects currently seen with known objects

within their database. They use omnimaper [27] as their mapping method and as a representation a combination of the downsampled voxel grids with additional normal and curvature information. Finally, all their operations are done in the non-planar components of the point cloud. Jensfelt et al [15] present an object based approach to SLAM where the robot can manipulate the objects of the map. They use camera pictures as input and receptive Field Histogram as the method to abstract the camera input and extract features for their object matching algorithm. Their approach is proposed as a solution to a service robot scenario. MonoSLAM [19] introduces a method of performing slam using a monocular camera.

What all those methods have in common is that they approach the problem of object based slam as a classification task. Objects need to be semantically understood before they are processed. The approach introduced in this paper considers the environment to be a collection of chunks. So having specific enough environment descriptors should lead to the robot being able to operate in an environment without having to explicitly label every object it encounters. This would remove the need of having to classify objects but would also increase the time it takes to extract features from the environment as features are the base of the unsupervised object discovery. Seongyong Koo et al. [20] introduce a method of unsupervised object individuation from RGB-D image sequences. They cluster their initial cloud into candidate objects using Eucledian clustering and proceed to extract features like the Euclidian distance(L2) and the Kullback-Leibler distance between point cloud objects. They use IMFT to solve their tracking problem.

2.2. Point Cloud Object segmentation

Research towards object segmentation in point clouds is focusing on calculating meta information regarding the points and applying a heuristic function to calculate if the points could belong in the same segment of the cloud. Trevor et al. [29] take positional information, Euclidean distances and the normal of points to as input to their heuristic and output segments that are part of the same object. PCL library [12] introduces methods like Euclidean clustering and conditional Euclidean clustering that use a number of heuristics that take normal as well as curvature information to extract segments in the point cloud that represent objects. Furthermore, a there is a lot of research on segmentation of point clouds in scenes, the emphasis is usually on extracting geometric primitives [30], [31] using cues like normals and curvature. Rabbani et al [23] introduce a new method of object segmentation using KNN as their base algorithm. They also present a very informative literature review along with the strengths and weaknesses of existing methods. Finally Triebel et al. [32] introduce a general clustering framework that does not rely on plane segmentation. Instead of segmenting the plane by using classical approaches like RANSAC or MLASAC they introduce a framework where they make no assumptions regarding plane data.

2.3. Non Parametric Bayesian methods

Bayesian non-parametric methods are the cornerstone of Bayesian statistics. In this project the focus was directed towards the clustering methods that are being introduced by those tools. Radford M. Neal [38] with his paper regarding MCMC methods for Dirichlet process mixture models made the definitive step towards Dirichlet process mixture models(DPMM's) receiving a lot of attention. Since then, a variety of approaches for inference on such models has been

introduced with Statistical inference and MCMC methods, and Variational inference being two prominent ones. Variational inference for DPMM's was introduced by Jordan et al. [39] and it introduces deterministic tools to perform inference and approximate the posterior distribution and marginals of a dataset. Both methods have strengths and weaknesses and many tools have been established by using the two approaches as their base. Blei et al. [43] introduced LDA as a method to perform topic modelling. Teh et al [41] introduce a hierarchy on the inference process by introducing the Hierarchical Dirichlet process. Particle filter approaches have also been established. Doucet et al. [42] introduce Sequential Monte Carlo as a fast way to approximate inference. Dirichlet process mixture models are a very active research field and covering it is beyond the scope of this report. In this project SMC samplers where used due to their robustness as well as their inherent extensiveness. A detailed description on the mechanisms of sequential samplers will be given in the theory section.

2.4. Correspondence

In its general definition, the correspondence problem refers to the problem of ascertaining which parts of one image correspond to which parts of another image, where differences are due to movement of the camera, the elapse of time, and/or movement of objects in the photos. Under the semantic SLAM context, it refers to the problem of identifying objects as objects that have been encountered before during the mapping process. Towards that direction Cree et al. [34] create a histogram of line segments of each landmark and compute their root mean square error. They then proceed to calculate their RGB signature to calculate the distance between different landmarks. Low et al. [35] match Scale Invariant Feature Transform (SIFT) features, an approach which transforms image data into scale-invariant coordinates relative to local features. Lamon et al [36] store a database of fingerprints which indicate the location in the robot's environment. The features are ordered and stored at a database at as they appear in the robot's immediate surroundings. A new fingerprint is computed for each new view and matched against existing ones. Finally, in Seghal et al. [37] an extension of SIFT descriptors to 3D data and point clouds is given.

The approach presented in this paper takes an input similar to [20] as parts of the point cloud are being clustered a mixture of distributions. The features that are used for the cloud representation are an extension of the features presented in [33] with the addition of angle information present in the points of the cloud. Since the operations are now done on cluster level, the distances among clusters can be then represented as distances between distributions and there has been extensive search on that field. Distances like Hellinger, KL divergence, Euclidian, Mahalanobis can all be taken into account when performing the object matching. The robustness of the method can also be increased by using tracking methods like IMFT. The novelty lies in its probabilistic mechanism as the clustering is done by using SMC to the augmented feature space. Using distributions as a means of representing objects within the point cloud is a form of compression as objects are represented by a distribution which is smaller in size and easier to maintain and expand.

3. Theory background

A basic background of GPU

3.1. Generalized Polya's Urn

Dirichlet process priors have been widely used in the literature as non parametric Bayesian tools to estimate the number of clusters in the data [46]. Dependent dirichlet processes extend those priors by allowing the clusters in the data to vary with some covariance over time. Dependent Dirichlet processes(DDP) remove the restriction of exchangeable data and introduce dependencies which can be temporal, positional etc. The DDPs are a natural extension of the DP's in domains where data cannot be considered exchangeable and have dependencies that cannot be disregarded. They where introduced by MacEachern [44] and have been widely used since. The main motivation behind using such methods is the immediate extension they provide to dynamic environments.

A DDP also known as Generalized Polya Urn [47] and has the property of randomly deleting partitions of clusters on every iteration. That way, it can cope with the variance of the data. In the current project, the n_th datapoint at time t,$x_{t,n}$ has an assignment $c_{t,n}$ at cluster $k \in \{1, 2, ..., K\}$. The size of cluster k at time t is defined as s_t^k. The GPU of this model at time t can now be defined as:

Algorithm 1 GPU

procedure GPU($pointCloud, t$)
  for $k = 1, ...K_{t-1,N_{t-1}}$ **do**
    Draw $\Delta s_{t-1}^k \sim Binom(s_{t-1,N_{t-1}}^k, \rho)$ ▷ Number of elements to delete
    Set $s_{t,0}^k = s_{t-1,N_{t-1}}^k - \Delta s_{t-1}^k$
  end for
  for $n = 1, ...N_t$ **do**
    Draw $c_{t,n} \sim Cat(\frac{s_{t,n-1}^1}{\alpha+\sum_k s_{t,n-1}^k}, \frac{s_{t,n-1}^{K_{t,n-1}}}{\alpha+\sum_k s_{t,n-1}^k}, \frac{\alpha}{\alpha+\sum_k s_{t,n-1}^k})$
    If $c_{t,n} \leq K_{t,n-1}$ *set* : $s_{t,n}^{c_t,n} = s_{t,n-1}^{c_t,n} + 1, K_{t,n} = K_{t,n-1}$
    If $c_{t,n} > K_{t,n-1}$ *set* : $s_{t,n}^{c_t,n} = 1, K_{t,n} = K_{t,n-1} + 1$
  end for
end procedure

Where Cat is a categorical distribution, Bin is the binomial distribution, α is the DP concentration parameter and ρ is the deletion parameter of the GPU. This Generative Polya Urn distribution also has the shorthand notation GPU(α, ρ)

This process can be though of in the terms of a general Chinese restaurant process as shown in Fig. 1. At time t (a), suppose there are customers seating at several tables in the restaurant. Each customer has to decide if he/she will remain at table with probability p or leave the restaurant with probability $1 - p$. Once all the customers make their decisions they leave the restaurant or remain seated (b). Each table occupied is moved according to the number of customers still seating in that table (c). A new customer then enters the table and either chooses to sit on one of

the existing tables (e) or choose a new with probability proportional to the strength parameter α of the model (f).

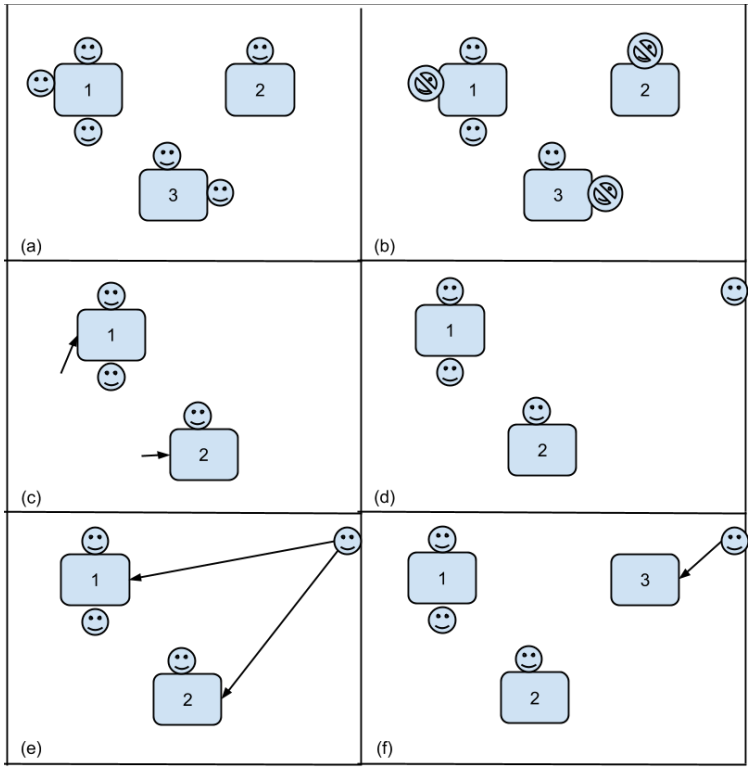

Figure 1: Generalised Polya Urn as presented in CRP.

4. Model definition

4.1. General pipeline

Now that the data distribution and sampler are defined, the model that takes as input point clouds from a Kinect sensor mounted on a robot and outputs the most probable landmarks given the input and the previous landmarks can be presented. Fig. 2 depicts the general workflow of what happens during the observation step of SLAM. The SLAM node– requires landmark information, and the landmark pipeline outputs the most probable landmarks given the current database of landmarks and the current observations. If needed landmarks added to the database and the landmark ids are given to back to the SLAM node.

The model introduces a Pipeline in the layer of landmark detection of the EKF-SLAM algorithm. All the operations from feature extraction to clustering and object matching will be performed at that layer. More specifically the pseudo-code for the method is the following:

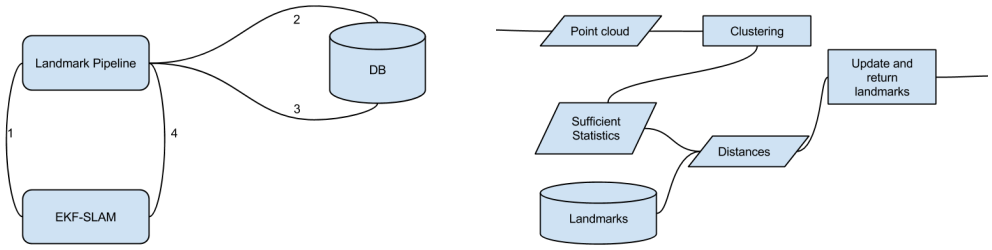

(a) General pipeline (b) Landmark pipeline

Figure 2: General landmark update pipeline

Algorithm 2 Landmark Layer

```
1:  procedure getLandmarkIds(pointCloud, timepoint, existingLandmarks) ▷ Post transformation
2:      initialize(landMarkIds)                                        ▷ Initialize empty list
3:      pointCloudReduced ← extractMetaFeatures(pointCloud)            ▷ Cloud preprocessing
4:      features ← extractMetaFeatures(pointCloudReduced)
5:      landmarks ← cluster(features)                                  ▷ Cluster using features
6:      for landmarks as landmark do
7:          (similarity, landId) ← calcBestSim(landmark, existingLandmarks)
8:          if similarity > threshold then
9:              addLandmarks(landMarkIds, landId)                      ▷ Return known landmark
10:         else
11:             newLandID ← addLandmarkDB(landmarkDB, landmark)        ▷ Add get new id
12:             addLandmarks(newLandID)                                ▷ Add landmark
13:         end if
14:     end for
15:     return landMarkIds                                             ▷ Return added landmark
16: end procedure
```

This top level description has a lot of implied steps so a line by line description will be provided:

Method input: The method takes as input a point cloud. The post transformation comment has to do with the fact that the cloud expected is the one after all the frame transformations are done in the tf layer of the robot.

Lines 3-4: Feature extraction is done through the pcl [12] library. An initial point cloud reduction is mandatory to increase the speed of the process. A voxel grid is used to reduce the dataset size. A leaf size of approximately 4cm produces a good tradeoff between precision and speed. The object representation approach is similar to [17]. Instead of using the CSHOT descriptor, pcl's fpfh [22] is being used. Fast point feature histogram(fpfh) represents an angular signature between a point and its neighbors. In that way we end up with a 23 dimensional angular signature of information between a point and its neighbors. Since the information are given in the form of a histogram, classical statistic solutions regarding the distances between angular signatures can be taken into account. In our solution EMD,Hellinger,and KL divergence are being computed in the pipeline. Color information is being encoded with an approach similar to [33]. The colour spectrum is discretized and what is extracted is the count of different colour signatures between a point and its k nearest neighbors. Finally positional information is also given as input to the algorithm. The pipeline is presented in figure Fig. 3. What the algorithm outputs is then a vector of $\mathbf{x} = (x_s, x_c, x_a)$ where s represents a 3x1 vector of space information, c a 27x1 vector of colour information and a angular information whose dimensionality depends on the distances computed(in our case 3x1). It must be noted that pcl offers a multi threading operation on the point feature histogram extraction. This feature is important since it greatly reduces(6-8 times) the speed of an operation applied on every point of the cloud and that makes the histogram extraction significantly faster.

Figure 3: Point cloud modification pipeline.

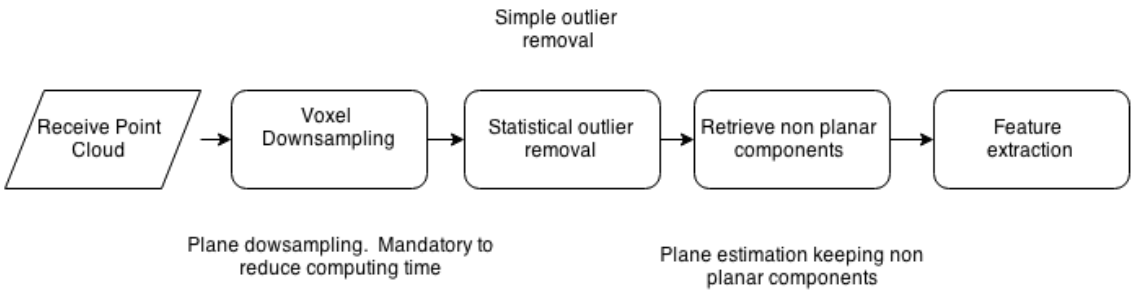

Lines 5: The clustering takes place in this line. The input of the method is the feature vector for every data point which is calculated in the previous steps. An SMC sampler is used as was presented in the theory section.

Lines 6-12: The correspondence of previously seen landmarks to current observations is computed in lines 6-12. Since the landmarks are distributions, statistical distances can be taken

to perform the matching. For every observation, its distances with all the stored landmarks are calculated. The calcBestSim function takes as input the observation and all the previously seen landmarks and returns highest similarity match with the landmarks already in the database as well as its landmark id. If the similarity is high enough, correspondence is performed and the landmark is added to the landmark list to be send for update in the EKF, otherwise a new landmark is added and its ID is then added to the list.

Lines 15: The algorithm returns the list of the most probable landmarks the robot encounters in this current time.

Now that the general pipeline is defined, specific parts of the method will be defined in more detail

4.2. The data distribution

The point cloud consists of many points hence a data unit will be considered a single point. Each point x in the input consists of a tuple $x = (x^s, x^a, x^c)$ where superscript s represents spatial information, a angle information, and c colour information. The method those features are extracted is explained in lines 3 and 4 in the general pipeline. For the purpose of this project each part of the cloud was represented by vector of length 32 with the first three elements representing the space information, elements 4-6 angle information, and the rest colour information.

The object model is a mixture of distributions over the data with each object beign modeled as $D(\theta_t^k)$ where θ represents the parameters of object k at time t. More specifically, each set **x** with n datapoints at time t is distributed as:

$$x_{t,n} \sim D(\theta_t^k) = Normal(x_{t,n}^s|\mu_t, \Sigma_t)Mult(x_{t,n}^c|\delta_t)Exp(x_{t,n}^a|\lambda_t)$$

Where Normal is a three dimensional Gaussian distribution with mean μ and covariance Σ representing the positional distribution of the data; Mult is a Categorical multinomial distribution with parameter vector δ representing weigths the colour distribution and Exp is an exponential with shape parameter λ representing the angle distribution of the data within the cluster. The exponential distribution was chosen to model angular information after empiric evaluation showed that it would be a good fit for the angle signature distribution of the data. A typical angle signature distribution is shown in. 4. For this graph data points from various point clouds where taken and passed through the pipeline analysed in lines 3-4. The data were then plotted, and the figure shows what the aggregated angle distribution between neighbor datapoints is. Since there is a clear exponential trend, the exponential distribution was chosen to model it. A gamma distribution is also a nice fit for the data, but due to time constrains, only one modeling distribution was explored.

Now that the distribution of the objects is defined, the progression of the sufficient statistics at time t given $t-1$ given by:

$$\theta_t^k|\theta_{t-1}^k \sim \begin{cases} T(\theta_{t-1}^k) & \text{if } k \leq K_{t-1} \\ G_0 & \text{if } k > K_{t-1}. \end{cases}$$

Where T represents the transition kernel of the data given the previous state in the model. The case $k > K_{t-1}$ represents the creation of a new cluster and G_0 is the base distribution of the DDP. In our case, the conjugate priors of the distributions of the data were chosen to model the base distribution. Therefore, G_0 is defined as:

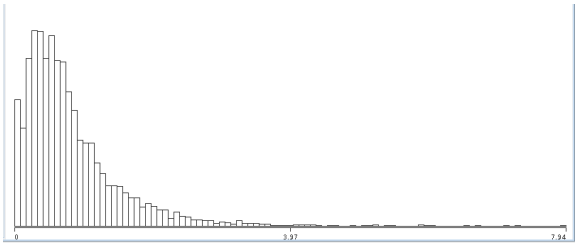

Figure 4: Exponential trend in KL distances.

$$G_0(\theta_t^k) = NiW(\mu_t^k, \Sigma_t^k | \kappa_0, \mu_0, \nu_0, \Lambda_0) Dir(\delta_t^k | q_0) Gam(\lambda_t^k | \alpha_0, \beta_0)$$

Where NiW is a Normal inverse Wishart distribution, Dir denotes a Dirichlet distribution, and Gam the Gamma distribution. $\kappa_0, \mu_0, \nu_0, \Lambda_0, q_0, \alpha_0$ and β_0 are predefined parameters of the model. The generative process for the Dependent Dirichlet mixture model can be written for each timestep t as:

---

1. Draw $c_t \sim GPU(\alpha, \rho)$
2. $\forall$ k draw: $\theta_t^k | \theta_{t-1}^k \sim \begin{cases} T(\theta_{t-1}^k) & \text{if } k \leq K_{t-1} \\ G_0 & \text{if } k > K_{t-1}. \end{cases}$
3. $\forall$ point n draw $x_{t,n} \sim F(\theta_t^{c_t,n})$

Given the theory in [47], the transition Kernel must satistfy:

$$\int G_0(\theta_k) T(\theta_t^k | \theta_{t-1}^k) d\theta_{t-1}^k = G_0(\theta_k)$$

The equation means that the invariant distribution must equal its base distribution. A typical way of meeting this restriction and forcing the sampler to converge to the original target density[49] is to introduce a set of M auxiliary variables $\mathbf{z}$ such that:

$$P(\theta_t^k | \theta_{t-1}^k) = \int P(\theta_t^k | z_t^k) P(z_t^k | \theta_{t-1}^k) dz_t^k$$

The transition kernel of the model can now be sampled by using the following formula $\theta_t^k \sim T(\theta_{t-1}^k) = T_2 \circ T_1(\theta_{t-1}^k)$ where:

$$\begin{aligned} z_t^k &\sim T_1(\theta_{t-1}^k) \\ &= Normal(\mu_{t-1}, \Sigma_{t-1}) Mult(\delta_{t-1}) Exp(\lambda_{t-1}) \end{aligned} \tag{1}$$

$$\begin{aligned} \mu_t, \Sigma_t, \delta_t, \lambda_t &\sim T_2(z_t^k) \\ &= NiW(\kappa_0, \mu_0, \nu_0, \Lambda_0) Dir(q_0) Gam(\alpha_0, \beta_0) \end{aligned} \tag{2}$$

where $\mu_t, \Sigma_t, \delta_t, \lambda_t$ are posterior parameters given the auxiliary variables z.

4.3. Sequential monte carlo sampler

Sequential monte carlo samplers for Dirichlet process mixture models where introduced by Doucet et al [50] and serve as fast alternative to MCMC and VI methods of performing posterior inference. SMC samplers have known strengths and weaknesses and are a good fit for the problem at hand, as their main theoretical disadvantage which is the particle degradation cannot occur in a time horizon of 1 that the sampler is being used. We can now define the SMC sampler that will be used to perform inference on our model as follows:

Algorithm 3 SMC for DDPM

Input: Points $\{x_{1,1:N_t}, ..x_{T,1:N_t}\}$with extracted features
Output: Clusters representing of the data
for $t = 1, ...T$ **do**
  for $l = 1, ...L$ **do**
    for $iter = 1, ...S$ **do**
      Sample $(c_t)^{(l)} \sim Q_1$
      Sample $(\theta^k) \sim Q_2$
    end for
  end for
  for $k = 1, ...K$ **do**
    Sample $\Delta s^k_{t-1} \sim Binom((s^k_{t-1,N_{t-1}})^{(l)}, \rho)$
    Set $s^k_{t,0} = s^k_{t-1,N_{t-1}} - \Delta s^k_{t-1}$
    Sample $((z^k_{t+1})^{(l)}) \sim T_1((\theta^k_t))^{(l)}$
  end for
  compute particle weights w^l_t
end for
Normalize and resample weights

4.3.1 Gibbs updates

The proposal distribution Q_1 is the probability of an assignment $c_{t,n}$ given cluster sizes, parameters and concentration α. Formally Q_1 can be written as:

$$Q_1(c_{t,n}|s^k_{t,n}, \theta^k_t, \alpha) \propto Cat(s^1_{t,n}, ...s^K_{t,n}, \alpha) \times \begin{cases} F(x_{t,n}|\theta^{c_t}_t) & \text{if } k \leq K_{t-1} \\ \int P(x_{t,n}|\theta_t)G_0(\theta)d\theta & \text{if } k > K_{t-1}. \end{cases} \tag{3}$$

Where $c_{t,n}$ represents cluster c of point n at time t, s represents cluster sizes. The integral represents the posterior predictive distribution of the cluster times the base distribution with the parameters integrated out. A review of the literature helps understand how the posterior predictive formula

is derived. More specifically, the analytic expression of the integral is:

$$\begin{aligned}\int P(x_{t,n}|\theta_t)G_0(\theta)d\theta = \int Normal(x^s_{t,n}|\mu_t,\Sigma_t)Mult(x^c_{t,n}|\delta_t)Exp(x^a_{t,n}|\lambda_t)\times \\ NiW(\mu_t,\Sigma_t|\kappa_0,\mu_0,\nu_0,\Lambda_0)Dir(\delta_t|q_0)Gam(\lambda_t|\alpha_0,\beta_0)d\theta \\ = \int Normal(x^s_{t,n}|\mu_t,\Sigma_t)\times NiW(\mu_t,\Sigma_t|\kappa_0,\mu_0,\nu_0,\Lambda_0) \\ Mult(x^c_{t,n}|\delta_t)\times Dir(\delta_t|q_0) \\ Exp(x^a_{t,n}|\lambda_t)\times\times Gam(\lambda_t|\alpha_0,\beta_0)d\theta \\ = t_{\nu_0-1}(x^s_{t,n}|\mu_0,\frac{\Lambda_0(\kappa_0+1)}{\kappa_0(\nu_0-1)})\times\prod_{j=1}^{V}\frac{\Gamma(x^c_{t,n})}{\Gamma(q_0)}\times \\ \frac{\Gamma(\sum_{j=1}^{V}q_0)}{\Gamma(\sum_{j=1}^{V}x^c_{t,n})}\times Lomax(\alpha_0+s^c_{t,n},\beta_0\sum_{j=1}^{V}x^c_{t,n})\end{aligned} \tag{4}$$

Where t represents student's t-distribution with ν degrees of freedom, Lomax represents Lomax distribution with shape and scale, α and β repsectively and the rest represent a Dirichlet-Multinomial(aka DirMul) distribution. The formulas of the posterior predictive distributions can be found in the literature with [48] being a good example.

The conjugacy of the base and prior distribution allows for an easy sampling formula for proposal distribution Q_2 which is of the form:

$$\begin{aligned}Q_2(\theta^k_t|\theta^k_{t-1},x^k_t,z^k_t)\propto F(x^k_t|\theta_k)\times T_2(\theta^k_t|z^k_t) \\ = NiW(\mu^k_t,\Sigma^k_t|\kappa_n,\mu_n,\nu_n,\Lambda_n)Dir(\delta^k_t|q_n)Gam(\lambda^k_t|\alpha_n,\beta_n)\end{aligned} \tag{5}$$

With:

$$\begin{aligned}\kappa_n &= \kappa_0+N \\ \nu_n &= \nu_0+N \\ \mu_n &= \frac{\kappa_0}{\kappa_0+N}\mu_0+\frac{N}{\kappa_0+N}\overline{x}^s \\ \Lambda_n &= \Lambda_0+s^s_x \\ q_N &= q_0+\sum_n x^c_i \\ \alpha_n &= \alpha_0+N \\ \beta_n &= \beta_0+\sum^n x^a_i\end{aligned} \tag{6}$$

Where $\overline{x}$ defines the sample mean for the elements assigned at cluster c, s_x the sample variance and N denotes the number of observations. The formulas for the updates can be found at the literature of cojugate priors with[52] being a good example.

4.3.2 Weight updates

The only thing left to explicitly define the sampler in its whole is the weight update step. More specifically, on every time step t the weight of particle l is calculated as:

$$w_t^{(l)} = \frac{P(c_t^{(l)}, \theta_t^{(l)}, x_t | \theta_{t-1})}{P(c_t^{(l)}, \theta_t^{(l)} | \theta_{t-1})} \tag{7}$$

Using bayes rule, the numerator can be written as:

$$P(x_t, | c_t^{(l)}, \theta_t^{(l)} \theta_{t-1}) \times P(c_t^{(l)}, \theta_t^{(l)} | \theta_{t-1}) \tag{8}$$

Which can be calculated using equations Q_2 and Q_1 for the first and second part respectively. After the particle weights are normalized particles are drawn with probability proportional to their weights.

4.4. Decision Layer

Once the sampler outputs the clusters of the point cloud the output can be passed to the decision layer. The question that the decision layer answers is: "How does the data/clusters I currently observe relate to the data I have previously seen in the past?". The decision of how an observation relates to previously encountered data has to be made and this decision is taken in the decision layer of the algorithm. To do that, distance measures must be defined between the observations and the landmarks. Distances between distributions are called divergences and a large amount of literature on divergences exists.

Since our data are modeled as comming from a convolution of 3 distributions, specific divergences for each part were considered. More specifically let l be the distribution of the landmark and o the distribution of the observation. l can be decomposed into 3 parts: l_G,l_C,l_E where G,C and E stand for Gaussian, Categorical and Exponential respectively. The observation distribution can be decomposed similarly. With that notation the distances between those distributions can be defined. For each individual landmark distribution l and observation distribution o the distances computed where the following:

- Gaussian
  - Wesserstein(l_G, o_G);
  - KL(l_G, o_G);
- Exponential
  - SquaredHellinger(l_E, o_E);
  - KL(l_E, o_E);
- Categorical
  - KL(l_C, o_C);

The decision boundary of an observation being a landmark or not was chosen by empiric evaluation of the landmarks. It is of course possible to learn the optimal decision boundary but due to time restrictions a simpler decision making approach was chosen instead.

4.5. Complexity

The complexity can be decomposed into three major parts. The cloud downsampling, the clustering and the decision making.

$$complexity = O(filter) + O(cluster) + O(decision)$$

Downsampling: The complexity of the cloud downsampling pipeline can be decomposed to the one of its components. This means that the decomposed complexity is defined as follows:

$$O(filter) = O(Vox\ Downsampling + Stat\ Removal + RANSAC + FPFH + Color\ estimation)$$

Voxel downsampling searches for neighbors within a distance defined by the user and keeps an average value that equally represents the cloud. Since the operation involves searching for neighbors of a point, and since search operations take $O(log\ n)$ time where N is the number of points within the cloud, the complexity of voxelGrid downsampling is $O(klogn)$ where k is the number of neighbors and n the number of points in the cloud. Statistial outlier removal searches for k nearest neigbhors and removes those whose deviation is passed a certain threshold. Given that search operations take $O(log\ n)$, for k neighbors, the complexity is $O(k\ log\ n)$. A high amount of research has been done regarding the optimal complexity of RANSAC [51]. RANSAC has a complexity of $O(k(t_M) + m_s * N)$ where k is the maximum amount of iterations defined by the user, m_s the average number of models per sample N the number of data points and t_M the time needed to draw a sample. The time variance also depends on the hardware. FPFH has a complexity of $O(nk)$ as given in [22]. Finally, for the operation of color estimation, the k nearest neighbors are chosen and some constant operation is performed on them. The complexity here is similar to Statistical outlier removal since operations after the search take a constant time $O(k\ log\ n)$ where k is the number of neighbors, n the number of points.

The downsampling pipeline has then a complexity of

$$O(filter) = O(k_0\ log\ n_{init} + k_1\ log\ n_1 + k_2(t_M) + m_s * n_2 + n_3 k_3 + k_4\ log\ n_3) \tag{9}$$

Different k indexes represent the number of neighbors defined for every operation. The n represents the number of points used as input. Using the notation of equation 9, n_{init} defines the whole cloud, n_1 the cloud after operation 1, n_2 the cloud after operations 2 etc.

Clustering: The complexity of the SMC sampler is defined in [33] as $O(TLKSN)$ where T defines the time frames, L the number of particles, K the number of clusters, S the number of samples, and N the size of the dataset. Given that the sampler is only used in single timesteps, the computational complexity is reduced to $O(LKSN)$. This is a low complexity and directly affects the performance since the sampler averages 10msec of excecution time.

$$O(cluster) = O(LKSN)$$

Decision making: The decision making takes $O(\kappa * l^2)$ computational time where κ defines the number of clusters output by the sampler and l the number of landmarks currently stored in the database. This number can be further reduced by taking for example only landmarks that are nearby the cluster, but optimizing the decision making performance is outside the scope of this project.

Finally, with some notation abuse, the final complexity of the method can then be defined as:

$$\begin{aligned} O(filter) + O(cluster) + O(decision) = \\ O(k_0 log n_0 + k_1 log n_1 + O(k_2(t_M) + m_s * n_2) + n_3 k_3 + k_4 log n_3) + O(LKSn_3) + O(\kappa * l^2) = \\ O(k_0 log n_0 + k_1 log n_1 + k_2(t_M) + m_s * n_2 + n_3 k_3 + k_4 log n_3 + LKSn_3 + \kappa * l^2) \end{aligned} \quad (10)$$

The complexity as defined in equation 10 depends greatly on the initial reduction of the voxel downsampling. As the voxel leaf size parameter decreases and the downsampling outputs a larger cloud, the precision as well as the computing time of the method increases. Since in this thesis the research was directed towards online SLAM methods, the leaf size was modified so that the cloud the time requirements for online landmark tracking were met.

4.6. Landmark size

The basic block of this algorithm is the cluster. In order to be able to compute how scalable the method is, the size of a single landmark will be computed. Each landmark is represetned by a single row in an SQLite database. To calculate how much space a landmark occupies, we will first calculate how space each of the columns has. Each row consists of 32 real numbers and 1 auto increment integer. Given that SQLite databases assign the memory dynamically, the worst case scenarios will be taken into account so that every other case is also included. According to the SQLite manual of datatypes [53] a real value takes up to 8 bytes of memory. An auto increment integer takes up to 4 bytes of information, so the total number of memory for a worst case scenario landmark is 260 bytes. This number can vary greatly over different environments and is a safe assumption to calculate the memory this method occupies.

5. Results

5.1. Simple datasets

In this section the performance and the output of the algorithm will be tested against a simple dataset. That will make the conceptual extension to more complex datasets that will be used in the robot easier. In order to test the sampling as well as the decision layer of the algorithm, a dataset provided by the pcl library was used. The reduced cloud as well as the cluster assignments color coded in the points are shown in Fig.5(a).

The cloud represents a milk cartridge transformed in two different positions. The pipeline will take the raw cloud as input, filter the cloud and pass it to the sampler to perform the clustering. Fig.5(b). The reduced point cloud is shown in the top left part of Fig.5(b). It is significantly smaller in size and this cloud along with all the meta-information needed are used to perform the clustering. The sampler outputs a mixture of distributions that best fits the data. The output of the

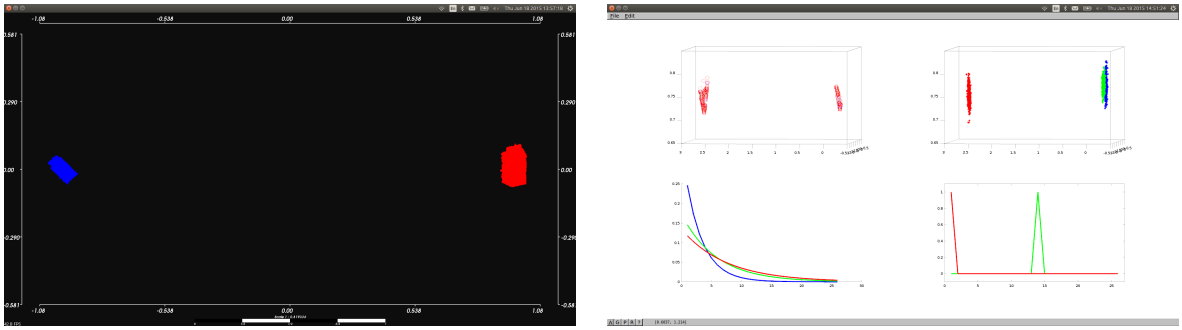

(a) Raw cloud (b) Post clustering

Figure 5: Initial data along with the distributions infered

cluster is shown in Fig.5(b) with the top right being the Gaussian distributions infered, bottom left the exponential and bottom right the categorical representing colour information of the cloud. The height of the objects leads to distribution with high variance in the z axis. The sampler outputs 3 clusters for the data and it can be seen that the change in angular information of the box leads the sampler to assign two distributions in the left milk box cloud. The colour information is captured correctly in the structures and that was expected since the data had distinct colour signatures.

UUID 2478					
LandUUID	GausKL	GausWes	ExpHel	ExpHel	CatKL
2478	0	1.18111e-07	0	0.164045	0
2479	0.0115821	53.5171	1.20726	0.319589	0
2480	13.5579	22449.9	1.56956	0.376699	13.8155
UUID 2479					
2478	0.0115821	20.1454	1.7215	0.319589	0
2479	5.42101e-20	4.88951e-08	0	0.411668	0
2480	12.8379	21458.6	0.474719	0.449769	13.8155
UUID 2480					
2478	13.5579	31191.5	2.55205	0.376699	13.8155
2479	12.8379	65013.8	0.53855	0.449769	13.8155
2480	0	2.43346e-07	0	0.481313	0

Now that the structured is infered, the ouput is given to the decision layer that calculates the distances between the clusters. The table shows the distances between the clusters infered. Having empiric results makes adding a simple decision boundary regarding an easier procedure. It can be seen that the first two landmarks have small distances in their Gaussian parts since they represent nearby areas of the cloud. The angular distance between them is large and that is why they form seperate clusters. The distinct colours of the milk make the colour signatures of the clusters distinct. An example with more complex colour signatures is shown in Fig.[6]. The clouds are now given a mixture of colours and this is passed to the color signature infered on every

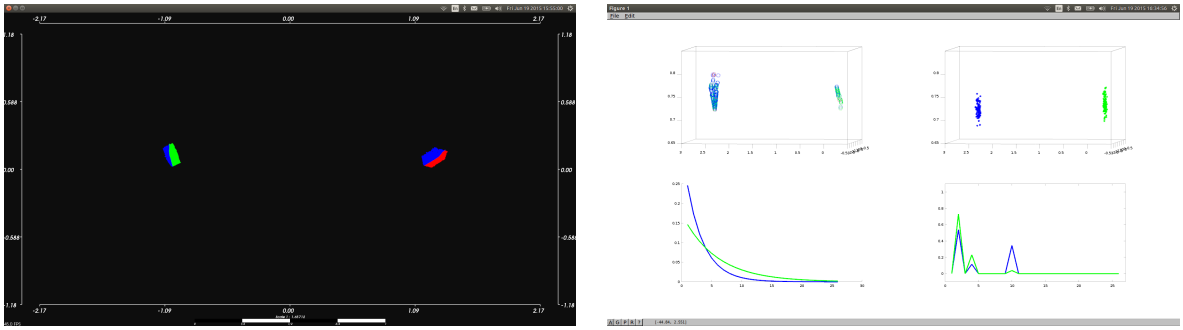

(a) Raw cloud (b) Post clustering

Figure 6: More complicated color distributions

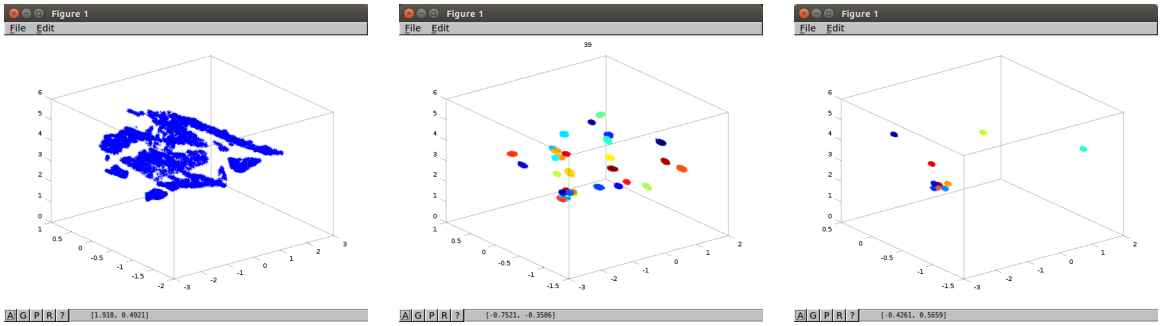

(a) Raw cloud (b) Post clustering (c) Landmark detection

Figure 7: Basic usage of the pipeline along with the clustering

cluster.

5.2. Offline testing

In the offline testing section, basic static results will be displayed and analyzed. The main purpose of the pipeline of Fig. 3 is to decrease the size of a point cloud so that operations on the reduced dataset are feasible. A point cloud instance as taken raw from the kinect sensor approximately 300.000 points and matrix operations at such large matrices are non feasible. The main target of the pipeline is to reduce the size of the data to a more manageable scale. The initial dense point cloud is shown in Fig. 7(a).

The raw cloud is too dense to be correctly displayed in the plot. The planar components of the plane also dominate the cloud and its hard to operate on them. An image with a high amount of planar components is typical when data are acquired from a turtlebot with the camera being situated near the ground. In order to perform the clustering operations, the cloud needs to be down-sampled. The process followed is the one described in the method definition and the results

are shown in Fig 7(b). The operation used is a pipeline voxel downsampling, statistical outlier removal and plane estimation via RANSAC is typical in the literature [20].

The cloud is stripped of its planar components with the remaining structure having minimal to no loss of structural information. The cloud is now ready to be used as input for the sampler which will take the features calculated in the pipeline to cluster the cloud into segments of structure. The whole takes a medium amount of time and depending on the parameter tweaking it can

The sampler as was described in the theory section takes as input the modified cloud and outputs clusters of the structure. Its results are shown in figure 7. The environment is captured as a sequence of clusters. It can be seen that the chair that is situated in the center of the cloud has a number of clusters assigned to it. This behavior of the cluster is expected as a lot of point clouds are part of the chair and the horizontal as well and the vertical components have different angular signatures. It is not possible to create a general framework that takes into account all the different angle and point signatures between objects. The decision of how the clusters represent a structure should then be taken in a decision layer on top of that cluster. A simple decision layer is implemented to classify objects by taking as input the output of the sampler.

The decision layer takes as input the distributions output by the sampler, and compares their characteristics to existing landmarks. Elements past a threshold are considered as landmarks already encountered; otherwise the new distributions are added to the database. The features taken by the algorithm are the distances between each distribution and each landmark already stored in the database. More specifically, for the Gaussian parts of the distribution Wasserstein and Kullback Leibler divergence are used to measure the distance between them. For the exponential part, squared Hellinger and Kullback-Leibler being used, and for the categorical EMD, KL divergence and Hellinger distance. All distribution distances are given in the appendix. The final result is a 7 feature vector that will be used to classify if it's a distance signature that classifies a landmark or not. The training set is supplied beforehand to the algorithm. The results of the algorithm are shown in Fig. 7

5.3. EKF-SLAM experiments

The method's results were given as input to an EKF-SLAM algorithm to test how it would perform using a point cloud as input. The results of feature extraction and cluster representation on simple objects like boxes are shown in the following figures.

As it is shown in the concentrated results that displays the features in combination with the point cloud, there is a large reduction in the dimensionality of the input. Given that a normal scene can be reproduced by an average of 20 clusters, and each cluster has a size of 256 bytes, the method is extremely scalable. Furthermore, the implementation can be extended to be even more performance based with techniques like recovering only the nearby clusters when searching for features, sorting the database or using parallel computing for optimal search time. Utilizing such tools can make the technique being able to handle a very large amount of features since 100.000 clusters can be used to represent large areas take only 256MB of space.

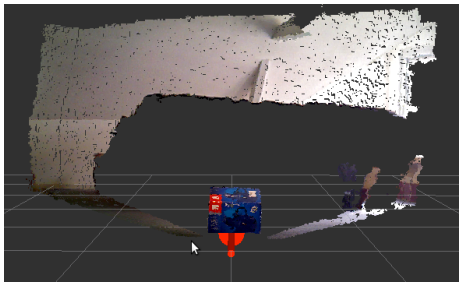

(a) Input

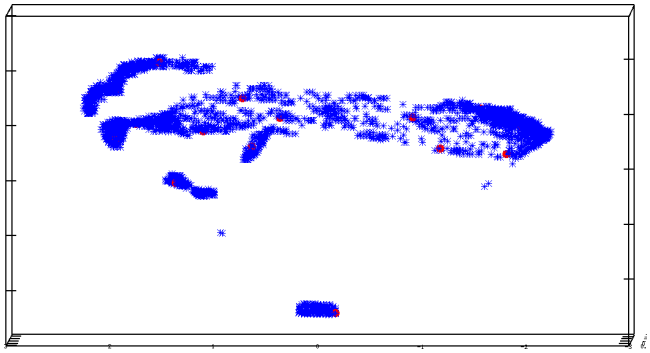

(b) Pointcloud along with landmarks

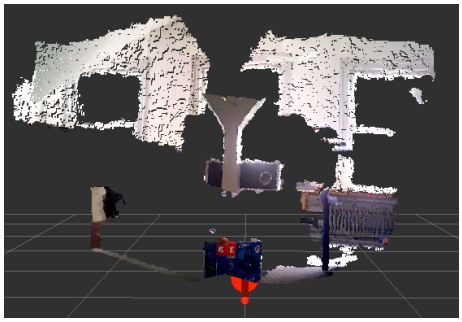

(c) Depth input

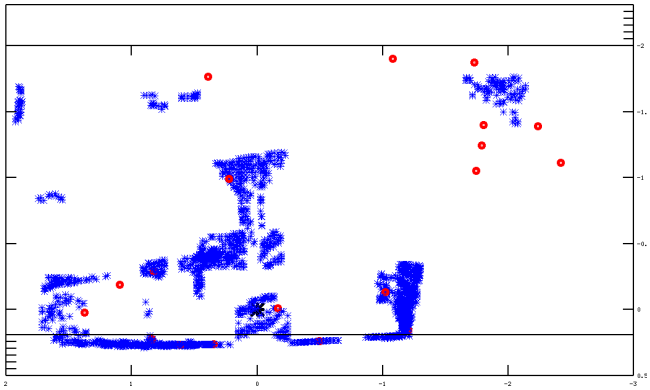

(d) Pointcloud along with landmarks

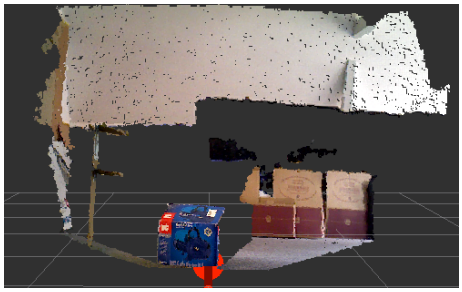

(e) Depth input

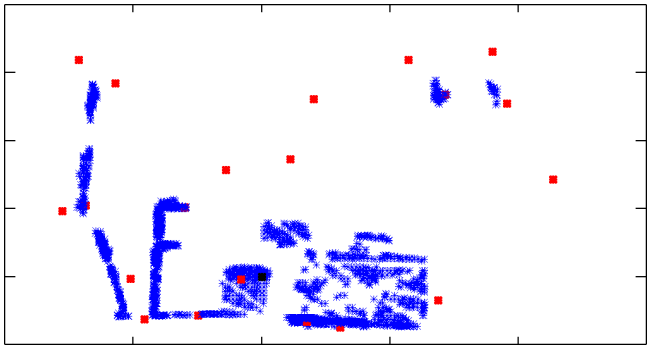

(f) Pointcloud along with landmarks

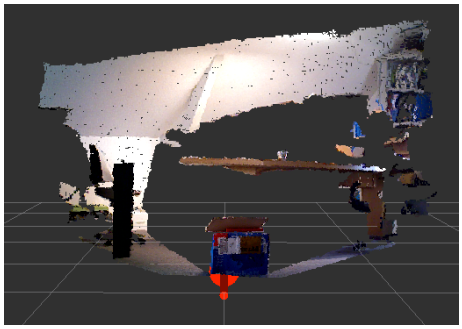

(g) Depth input

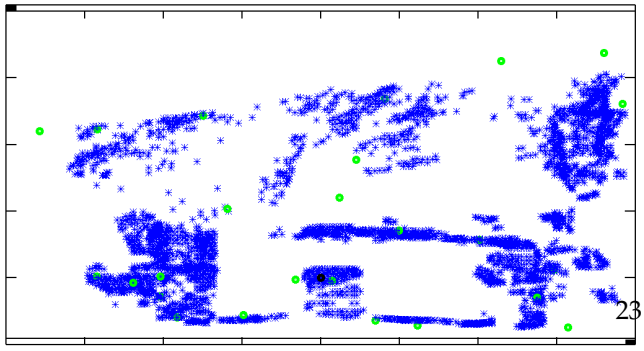

(h) Pointcloud along with landmarks

Figure 8: caption

6. Conclusion and future work

A novel method for SLAM by using compressed representations of objects in a point cloud is introduced. Its strengths and weaknesses are presented. Future work could include:

- Improved tracking by using IMRF
- Extend to dynamic environments
- Extend the representation used

7. Discussion

A fast method of pointcloud clustering and representation are presented. Its strengths and weaknesses are given. This method serves as a proof of concept on how non-parametric bayesians could help

References

[1] Thrun, S. (2002). Probabilistic robotics. Communications of the ACM, 45(3), 52-57.

[2] Bailey, T., Nieto, J., Guivant, J., Stevens, M., & Nebot, E. (2006, October). Consistency of the EKF-SLAM algorithm. In Intelligent Robots and Systems, 2006 IEEE/RSJ International Conference on (pp. 3562-3568). IEEE.

[3] Thrun, S., & Montemerlo, M. (2006). The graph SLAM algorithm with applications to large-scale mapping of urban structures. The International Journal of Robotics Research, 25(5-6), 403-429.

[4] Figueredo, A.J. and Wolf, P. S.A. (2009). Assortative pairing and life history strategy - a cross-cultural study. *Human Nature*, 20:317–330.

[5] Thrun, S., & Mitchell, T. M. (1995). Lifelong robot learning. The Biology and Technology of Intelligent Autonomous Agents, 165-196.

[6] Konolige, K., & Bowman, J. (2009, October). Towards lifelong visual maps. In Intelligent Robots and Systems, 2009. IROS 2009. IEEE/RSJ International Conference on (pp. 1156-1163). IEEE.

[7] Walcott, A. (2011). Long-term robot mapping in dynamic environments (Doctoral dissertation, Massachusetts Institute of Technology).

[8] Hjort, N. L., Holmes, C., MÃijller, P., & Walker, S. G. (Eds.). (2010). Bayesian nonparametrics (Vol. 28). Cambridge University Press.

[9] MacEachern, S. N. (2000) Dependent dirichlet processes. Unpublished manuscript, Department of Statistics, The Ohio State University.

[10] Barber, D. (2012) Bayesian reasoning and machine learning.

[11] Neiswanger, W., Wood, F., & Xing, E.The dependent dirichlet process mixture of objects for detection-free tracking and object modeling. In Proceedings of the Seventeenth International Conference on Artificial Intelligence and Statistics (pp. 660-668) (2014, August)

[12] Rusu, R. B., & Cousins, S. (2011, May). 3d is here: Point cloud library (pcl). In Robotics and Automation (ICRA), 2011 IEEE International Conference on (pp. 1-4). IEEE.

[13] LabbÃl', M., & Michaud, F. (2011, September). Memory management for real-time appearance-based loop closure detection. In Intelligent Robots and Systems (IROS), 2011 IEEE/RSJ International Conference on (pp. 1271-1276). IEEE.

[14] Salas-Moreno, R. F., Newcombe, R. A., Strasdat, H., Kelly, P. H., & Davison, A. J. (2013, June). Slam++: Simultaneous localisation and mapping at the level of objects. In Computer Vision and Pattern Recognition (CVPR), 2013 IEEE Conference on (pp. 1352-1359). IEEE.

[15] Selvatici, A. H., & Costa, A. H. (2008). Object-based visual slam: How object identity informs geometry.

[16] Castle, R. O., Gawley, D. J., Klein, G., & Murray, D. W. (2007, April). Towards simultaneous recognition, localization and mapping for hand-held and wearable cameras. In Robotics and Automation, 2007 IEEE International Conference on (pp. 4102-4107). IEEE.

[17] Choudhary, S., Trevor, A. J., Christensen, H. I., & Dellaert, F. (2014, September). SLAM with object discovery, modeling and mapping. In Intelligent Robots and Systems (IROS 2014), 2014 IEEE/RSJ International Conference on (pp. 1018-1025). IEEE.

[18] Jensfelt, P., Ekvall, S., Kragic, D., & Aarno, D. (2006, September). Augmenting slam with object detection in a service robot framework. In Robot and Human Interactive Communication, 2006. ROMAN 2006. The 15th IEEE International Symposium on (pp. 741-746). IEEE.

[19] Davison, A. J., Reid, I. D., Molton, N. D., & Stasse, O. (2007). MonoSLAM: Real-time single camera SLAM. Pattern Analysis and Machine Intelligence, IEEE Transactions on, 29(6), 1052-1067.

[20] Koo, S., Lee, D., & Kwon, D. S. (2014, September). Unsupervised object individuation from RGB-D image sequences. In Intelligent Robots and Systems (IROS 2014), 2014 IEEE/RSJ International Conference on (pp. 4450-4457). IEEE.

[21] Cichocki, A., & Amari, S. I.Families of alpha-beta-and gamma-divergences: Flexible and robust measures of similarities. Entropy, 12(6), 1532-1568.

[22] Fast point feature histogram.Rusu, R. B., Blodow, N., & Beetz, M. (2009, May). Fast point feature histograms (FPFH) for 3D registration. In Robotics and Automation, 2009. ICRA'09. IEEE International Conference on (pp. 3212-3217). IEEE.

[23] Rabbani, T., van den Heuvel, F., & Vosselmann, G. (2006). Segmentation of point clouds using smoothness constraint. International Archives of Photogrammetry, Remote Sensing and Spatial Information Sciences, 36(5), 248-253.

[24] Caron, F., Davy, M., & Doucet, A. (2012) Generalized Polya urn for time-varying Dirichlet process mixtures. arXiv preprint arXiv:1206.5254.

[25] Zhang, Z. (2012) Microsoft kinect sensor and its effect. MultiMedia, IEEE, 19(2), 4-10.

[26] Wainwright, M. J., & Jordan, M. I. (2008). Graphical models, exponential families, and variational inference. Foundations and Trends in Machine Learning, 1(1-2), 1-305. "

[27] A.Trevor, J.Rogers, and H.Christensen. Omnimapper: A modular multimodal mapping framework. In IEEE International Conference on Robotics and Automation (ICRA), 2014

[28] Koo, S., Lee, D., & Kwon, D. S. (2013, November). Multiple object tracking using an rgb-d camera by hierarchical spatiotemporal data association. In Intelligent Robots and Systems (IROS), 2013 IEEE/RSJ International Conference on (pp. 1113-1118). IEEE.

[29] Trevor, A. J., Gedikli, S., Rusu, R. B., & Christensen, H. I. (2013). Efficient organized point cloud segmentation with connected components. Semantic Perception Mapping and Exploration (SPME).

[30] Unnikrishnan, R., & Hebert, M. (2003, October). Robust extraction of multiple structures from non-uniformly sampled data. In Intelligent Robots and Systems, 2003.(IROS 2003). Proceedings. 2003 IEEE/RSJ International Conference on (Vol. 2, pp. 1322-1329). IEEE.

[31] Rabbani, T., van den Heuvel, F., & Vosselmann, G. (2006). Segmentation of point clouds using smoothness constraint. International Archives of Photogrammetry, Remote Sensing and Spatial Information Sciences, 36(5), 248-253.

[32] Triebel, R., Shin, J., & Siegwart, R. (2010, June). Segmentation and unsupervised part-based discovery of repetitive objects. In Robotics: Science and Systems (Vol. 2).

[33] Neiswanger, W., Wood, F., & Xing, E. (2014, August). The dependent dirichlet process mixture of objects for detection-free tracking and object modeling. In Proceedings of the Seventeenth International Conference on Artificial Intelligence and Statistics (pp. 660-668).

[34] Cree, M. J., Jefferies, M. E., & Baker, J. T. Using 3D Visual Landmarks to Solve the Correspondence Problem in Simultaneous Localisation and Mapping.

[35] Lowe, D. G. (2004). Distinctive image features from scale-invariant keypoints. International journal of computer vision, 60(2), 91-110.

[36] Lamon, P., Tapus, A., Glauser, E., Tomatis, N., & Siegwart, R. (2003, October). Environmental modeling with fingerprint sequences for topological global localization. In Intelligent Robots and Systems, 2003.(IROS 2003). Proceedings. 2003 IEEE/RSJ International Conference on (Vol. 4, pp. 3781-3786). IEEE.

[37] Sehgal, A., Cernea, D., & Makaveeva, M. (2010). Real-time scale invariant 3D range point cloud registration. In Image Analysis and Recognition (pp. 220-229). Springer Berlin Heidelberg.

[38] Neal, R. M. (2000). Markov chain sampling methods for Dirichlet process mixture models. Journal of computational and graphical statistics, 9(2), 249-265.

[39] Blei, D. M., & Jordan, M. I. (2006). Variational inference for Dirichlet process mixtures. Bayesian analysis, 1(1), 121-143.

[40] Montemerlo, M., Thrun, S., Koller, D., & Wegbreit, B. (2002). FastSLAM: A factored solution to the simultaneous localization and mapping problem. AAAI/IAAI, 593-598.

[41] Teh, Y. W., Jordan, M. I., Beal, M. J., & Blei, D. M. (2006). Hierarchical dirichlet processes. Journal of the american statistical association, 101(476).

[42] Doucet, A., De Freitas, N., & Gordon, N. (2001). An introduction to sequential Monte Carlo methods (pp. 3-14). Springer New York.

[43] Blei, D. M., Ng, A. Y., & Jordan, M. I. (2003). Latent dirichlet allocation. the Journal of machine Learning research, 3, 993-1022.

[44] MacEachern, S. N. (2000). -

[45] Fox, E. B., Sudderth, E. B., Jordan, M. I., & Willsky, A. S. (2011). A sticky HDP-HMM with application to speaker diarization. The Annals of Applied Statistics, 5(2A), 1020-1056.

[46] Charles E Antoniak,Mixtures of dirichlet processes with applications to bayesian nonparametric problems, The annals of statistics (1974), 1152âĂŞ1174

[47] F. Caron, M. Davy, and A. Doucet, Generalized Polya urn for time-varying Dirichlet process mixtures, 23rd Conference on Uncertainty in Artificial Intelligence (UAIâĂŹ2007), Vancouver, Canada, July 2007, 2007

[48] Fink, D. (1997). A compendium of conjugate priors.

[49] ÃIJlker, Y., GÃijnsel, B., & Cemgil, A. T. (2010). Sequential Monte Carlo samplers for Dirichlet process mixtures. In International Conference on Artificial Intelligence and Statistics (pp. 876-883).

[50] Del Moral, P., Doucet, A., & Jasra, A. (2006). Sequential monte carlo samplers. Journal of the Royal Statistical Society: Series B (Statistical Methodology), 68(3), 411-436.

[51] Meer, P., Mintz, D., Rosenfeld, A., & Kim, D. Y. (1991). Robust regression methods for computer vision: A review. International journal of computer vision, 6(1), 59-70.

[52] Raiffa, H. (1974). Applied statistical decision theory.

[53] https://www.sqlite.org/datatype3.html